

# Interaction of oxygen with Al(111) at elevated temperatures

J. Trost,<sup>a)</sup> H. Brune,<sup>a)</sup> J. Winterlin,<sup>b)</sup> R. J. Behm,<sup>c)</sup> and G. Ertl  
*Fritz-Haber-Institut der Max-Planck-Gesellschaft, Faradayweg 4-6, 14195 Berlin, Germany*

(Received 10 July 1997; accepted 15 October 1997)

The interaction of oxygen with Al(111) was investigated by STM at temperatures between 350 and 530 K, by annealing an oxygen precovered surface and by adsorption of oxygen on the hot surface. For exposures up to 10 L and temperatures up to 470 K a considerable part of the oxygen exists still in the chemisorbed state, another part transforms into Al oxide. In contrast to 300 K chemisorbed  $O_{ad}$  atoms are mobile at elevated temperatures, and compact, hexagonal  $(1 \times 1)O_{ad}$  islands develop by an ordinary nucleation and growth scheme. This evidences attractive interactions between the oxygen atoms on  $(1 \times 1)$  sites. From the lateral distribution of  $O_{ad}$  islands a diffusion barrier of 1.0–1.1 eV is derived. The imaging of the islands of the  $(1 \times 1)$  phase by STM depends on their size, which is understood by a different imaging of the  $O_{ad}/Al$  adsorbate complexes at the island borders. Defects in the islands and bright features at the edges are interpreted as nuclei of aluminum oxide. Additional features which appear as topographic holes may be attributed to nonconducting Al oxide grains. © 1998 American Institute of Physics. [S0021-9606(98)01204-5]

## I. INTRODUCTION

In this paper we present STM (scanning tunneling microscopy) results about the interaction of  $O_2$  with Al(111) at elevated temperatures, thereby completing our former studies that were restricted to room temperature.<sup>1,2</sup> At 300 K the chemisorption of oxygen on Al(111) was found to be characterized by unique nonequilibrium effects. It was suggested that the dissociation into  $O_{ad}$  proceeds via “hot” atoms, displaying an extreme, nonthermal mobility in the short time interval after dissociation during which the adsorption energy is released to the heat bath of the substrate. (This interpretation is under discussion at present, see Refs. 3–5.) On the other hand, the thermal mobility, after equilibration, is basically zero. Both effects are connected with the large binding energy between the chemisorbed oxygen atoms and the aluminum surface (a recent calculation revealed 5 eV per atom with respect to the free  $O_2$  molecule<sup>5</sup>), because it determines the maximum kinetic energy of the hot atoms, but governs also the diffusion barrier  $E_{diff}^*$  which is often a fixed fraction of the adsorption energy.<sup>6</sup> From the value of about 1 eV that was estimated for  $E_{diff}^*$  previously<sup>2</sup> the oxygen atoms should become mobile at  $T > 300$  K and the structure of the adsorption layer be determined more by its thermodynamic stability than by kinetic effects. It was hoped therefore that by experiments at elevated temperatures more insight into the energetics of the O/A(111) system could be gained.

In short, at 300 K the interaction of  $O_2$  with Al(111) proceeds in two steps as a function of coverage (see Ref. 2 and the references cited therein):

- ◆ At small coverages islands with a  $(1 \times 1)$  structure of chemisorbed oxygen are formed.<sup>2</sup> The recent work<sup>5,7,8</sup>

agrees that the oxygen atoms occupy threefold coordinated sites at the fcc (face-centered-cube) position, 0.7 Å above the Al surface plane. An additional subsurface oxygen species had been discussed extensively in earlier publications.<sup>9</sup> Based on the present knowledge, such a species appears to be unlikely, and in the previous STM study<sup>2</sup> a second chemisorbed species was not detected, although STM has proven to be sensitive to subsurface features.<sup>10</sup> At 300 K island nuclei consist of only one atom. The islands grow only slowly with coverage, because of the rapid nucleation of new islands. That the islands grow at all, despite of the thermal immobility of the  $O_{ad}$  atoms, was explained by trapping of hot atoms near already thermalized atoms. At intermediate coverages the small oxygen islands coalesce which leads to a network of irregular dark spots in the STM images (Figs. 13 and 14 in Ref. 2). In agreement with theory<sup>11</sup> oxygen is imaged dark for most tunneling parameters, i.e., as a depression.

- ◆ At an  $O_{ad}$  coverage of about 0.2, i.e., when a large fraction of the surface is still empty, oxidation starts. It is characterized by the development of small bright features in the STM topographs, identified with oxide grains by the simultaneous detection of the  $Al_{L_{VV}}$  Auger transition at 54 eV characteristic of aluminum oxide.<sup>2</sup> The oxide grains nucleate predominantly at the perimeters of oxygen islands and at step edges. Upon further oxygen exposure the oxidation proceeds by formation of additional oxide grains, until the surface is completely covered with a disordered layer of oxide nuclei.

Knowledge about the adsorption behavior of  $O_2$  on Al(111) at elevated temperatures is so far based on a number of spectroscopic studies in which the surface was precovered at 300 K or lower temperatures and then annealed. Using x-ray photoemission spectroscopy (XPS), the  $O(1s)$  peak<sup>12</sup> was found to show similar changes as when the surface was exposed to larger amounts of  $O_2$  at room temperature; the

<sup>a)</sup>Present address: Institut de Physique Expérimentale, EPFL-PHB-Écublens, 1015 Lausanne, Switzerland.

<sup>b)</sup>Author to whom correspondence should be addressed.

<sup>c)</sup>Present address: Abt. Oberflächenchemie und Katalyse, Universität Ulm, 89069 Ulm, Germany.

Al(2p) state<sup>13-16</sup> showed a shift by 2.7 eV towards higher binding energy characteristic for the oxide (which can be clearly discriminated from the 1.4 eV shifted, chemisorbed state), and high-resolution electron energy loss spectroscopy (HREELS)<sup>17,18</sup> revealed the typical oxidic three peak spectrum. All of these data seem to indicate that upon annealing the chemisorbed oxygen layer just transforms into Al oxide.

## II. EXPERIMENT

The experiments were performed in an ultrahigh vacuum (UHV) system containing the STM that was described in detail in an earlier paper.<sup>2</sup> The system is equipped also with facilities for Auger electron spectroscopy (AES), low energy electron diffraction (LEED), sputter cleaning and annealing of the sample; the base pressure is below  $1 \times 10^{-10}$  Torr. STM images were recorded at room temperature; image sizes, tunneling voltages, and currents are given at each figure, with the sample bias with respect to the tip potential. For details about the sample preparation we refer to the previous publication.<sup>2</sup>

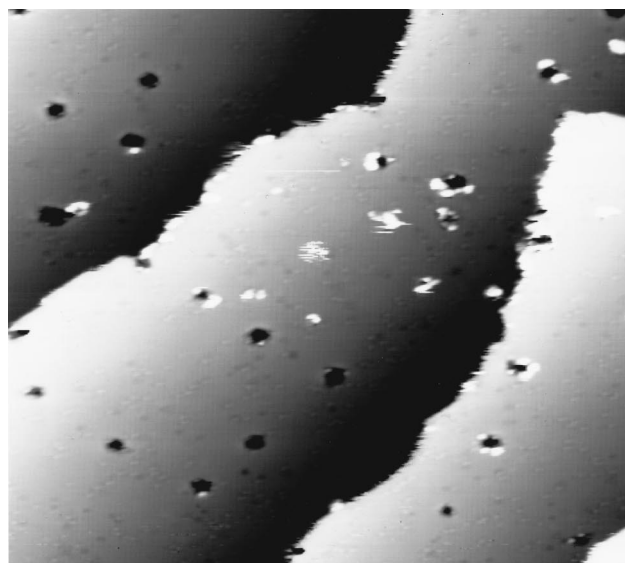
## III. RESULTS

### A. Nucleation and growth during annealing

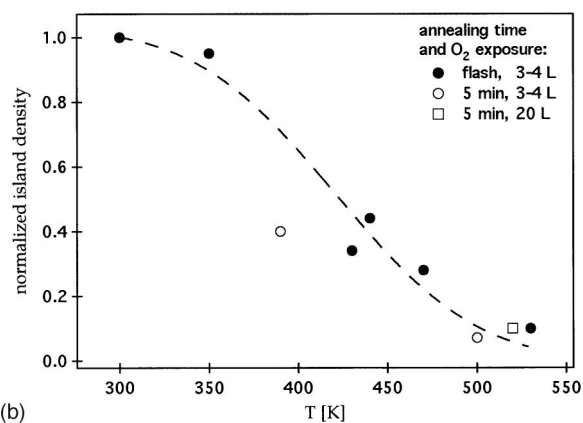
In one set of experiments oxygen was adsorbed at 300 K and then annealed at higher temperatures. As was shown in our previous publication (Fig. 12 of Ref. 2) small exposures at room temperature create very small clusters of chemisorbed oxygen; for example, an exposure of 3 L of O<sub>2</sub> leads to about 90% single atoms and 10% dimers, and (counting each separate atom or cluster as an island) to a density of islands of 0.0069 with respect to the number of surface aluminum atoms. After annealing to 530 K the STM image shown in Fig. 1(a) was recorded. The terraces are covered with dark islands, some of them decorated with bright spots. The island density has decreased, in this case to  $\rho = 0.0011$ , i.e., by a factor of 6 compared to the situation before the annealing. At the same time the islands have significantly grown as compared to the single and double atom features found at room temperature so that the total area covered by oxygen is roughly constant. This indicates that the majority of the oxygen atoms is still present on the surface, consistent with the unchanged AES O<sub>KLL</sub> signal, from which we conclude that neither significant diffusion into the bulk nor desorption takes place under these conditions.

Figure 1(b) collects the results from several annealing experiments, showing island densities, normalized to the respective room temperature value, as a function of temperature; as additional parameters oxygen exposures and annealing times were varied. The island density starts to decrease at 350 K, and is about 10% of the initial value at 500 K; annealing at higher temperatures does not lead to a further change. The annealing time (up to 5 min) and oxygen exposure (up to 20 L) have only little effect.

These experiments have several implications for the chemical nature and the characteristics of the oxygen atoms involved in the processes at higher temperatures: That the



(a)



(b)

FIG. 1. (a) STM topographs of Al(111) after exposure to 3 L O<sub>2</sub> and annealing at 530 K ( $433 \text{ \AA} \times 411 \text{ \AA}$ ,  $-1.0 \text{ V}$ ,  $2 \text{ nA}$ ). (b) Normalized island density vs annealing temperature for various annealing times and O<sub>2</sub> exposures; broken line only to guide the eye.

islands grow between 350 and 500 K requires surface diffusion of the oxygen atoms. From the temperatures and the corresponding island densities rough estimates of the diffusion barrier can be performed. Assuming that the island density reflects the inverse of the squared diffusion length and setting  $D_0$  equal to  $5 \cdot 10^{-3} \text{ cm}^2 \text{ s}^{-1}$  reveals a value of 1.0 eV at 440 K for  $E_{\text{diff}}^*$ . This value is consistent with the minimum barrier of 1.0 eV that was derived from the thermal immobility of O<sub>ad</sub> at 300 K,<sup>2</sup> indicating that the rate limiting step for the island density decrease during the annealing is the diffusion of O<sub>ad</sub> atoms.

The fact that the island density decreases by annealing also after somewhat larger exposures, at which islands are present already at 300 K, means furthermore that the O<sub>ad</sub> clusters formed at room temperature can dissolve again. After an exposure of 20 L at 300 K more than half of the islands consist of several atoms,<sup>2</sup> which means that islands containing at least three atoms dissolve completely. Hence, at temperatures  $\geq 350 \text{ K}$  oxygen atoms detach from islands,

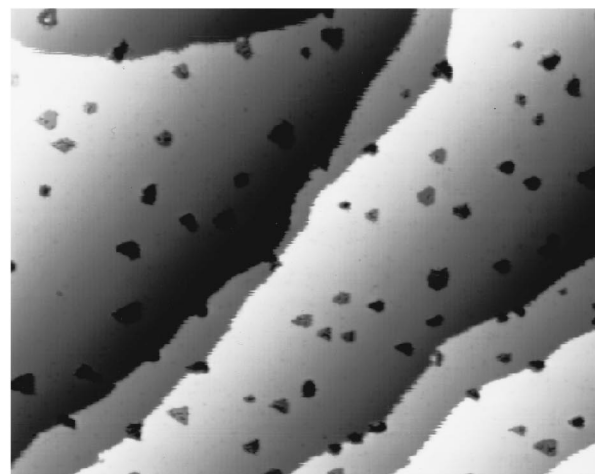
diffuse across the surface and are incorporated into larger islands, equivalent to an Ostwald ripening process. This further supports our previous interpretation of the  $(1 \times 1)O$  structure consisting of oxygen atoms chemisorbed on surface rather than on subsurface sites. It is also in agreement with the more recent structural studies on this subject<sup>5,7,8,19</sup> and with the fact that the diffusion barrier has the expected value for a surface species. If, in contrast, the oxygen atoms had moved to subsurface sites already at 300 K, it does not appear very likely that they would jump back to sites on the surface by annealing and travel across the terraces to form larger islands; in this case one would rather expect them to move to deeper layers as is known from other systems.<sup>20</sup>

That the island density is not reduced further than to about 10% of its initial value by annealing above 500 K indicates, however, that, in addition to Ostwald ripening, a second process takes place. This is attributed to a conversion of the islands into a more stable structure that prevents dissolution. The most natural interpretation is the transformation into aluminum oxide which is suggested also by the protrusions in Fig. 1(a) which are mostly located near the island borders. These features are very similar to the oxide nuclei formed at 300 K,<sup>2</sup> and presumably represent the same chemical species. Identification by AES is hampered by their low density.

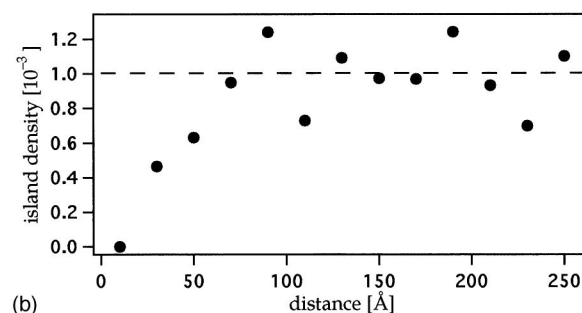
In a second set of experiments oxygen was adsorbed directly at elevated temperatures. Figure 2(a) shows an STM topograph recorded after an exposure of 3 L of  $O_2$  at 440 K. The dark islands on the terraces cover about 4% of the surface area; their mean diameter of about 20 Å is again significantly larger than for room-temperature adsorption. The island density is 0.001, i.e., by a factor of 3 smaller than when the same amount of oxygen was adsorbed at room temperature followed by annealing at 440 K.

This difference can be rationalized as follows. Room-temperature adsorption yields very small islands, e.g., at an exposure of 3 L predominantly monomers. When this surface is annealed, all monomers become mobile at the same time leading to a high density of atoms and hence a small mean free path. This results in a large formation rate of nuclei and a relatively large island density. On the other hand, for adsorption at elevated temperatures the adatoms are immediately mobile and encounter other atoms to form nuclei after times generally much smaller than the deposition time. The monomer density remains therefore small so that the mean free path is larger and the resulting island density smaller.

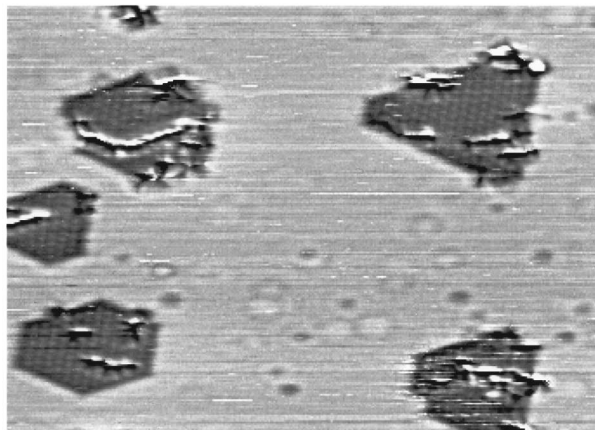
Most of the islands in Fig. 2(a) are spread evenly over the terraces suggesting homogeneous nucleation. However, there are also several islands directly at steps. In order to make a quantitative comparison between the nucleation probabilities at the steps and the terraces the mean distance between the islands along the steps was evaluated and compared to the mean distance between islands along randomly chosen lines. It is found that the islands along the steps are closer together on the average, by factor of more than 2, than along arbitrary lines. This indicates that, although the majority of the islands is formed by homogeneous nucleation on



(a)



(b)



(c)

FIG. 2. (a) Al(111) surface after an  $O_2$  exposure of 3 L at 440 K.  $864 \text{ \AA} \times 679 \text{ \AA}$ ;  $-0.9 \text{ V}$ ,  $0.23 \text{ nA}$ . (b) Island density in (a) as a function of distance from center islands; the dashed line shows the mean value. (c) Topograph after exposure of 5 L  $O_2$  at 470 K.  $140 \text{ \AA} \times 116 \text{ \AA}$ ,  $-0.75 \text{ V}$ ,  $1 \text{ nA}$ .

the terraces, there is a somewhat larger probability for heterogeneous nucleation at the atomic steps.

Information about the island growth is gained from the spatial distribution of the islands, by analysis of the island density as function of distance from given islands, and taking the average over all islands as centers. The result for the STM image of Fig. 2(a) is shown in Fig. 2(b). It is found that the density is smaller than the mean value of  $\rho=0.001$  (dashed line) in a zone of about 70 Å around the islands; at larger distances the data scatter randomly around the mean

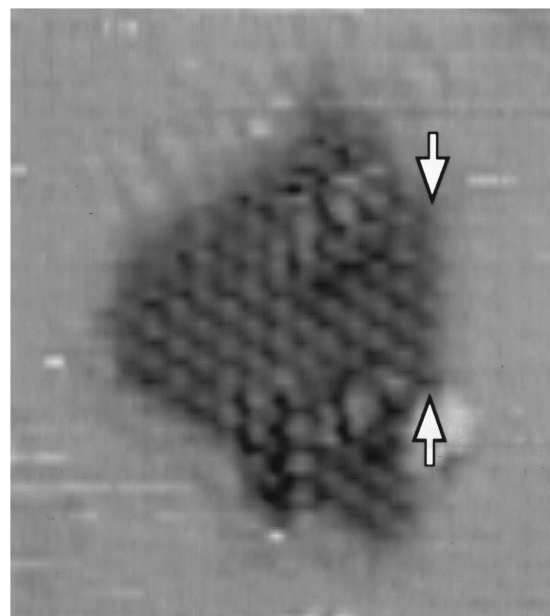
value. Depletion zones are characteristic for nucleation in epitaxy<sup>21</sup> and for precipitation processes in three-dimensional alloys<sup>22</sup> and are well understood. They occur around islands and precipitations in those cases where particle diffusion is the rate limiting step of the growth. Following this interpretation the reduced island density is caused by an oxygen concentration profile building up around a growing center island that acts as a sink for diffusing oxygen atoms. This reduces the  $O_{ad}$  coverage around that island and thereby the nucleation probability for further islands. The radius of the depletion zone allows also a more precise estimate of the diffusion barrier. Setting the diffusion length equal to the radius of the depletion zone of 70 Å and assuming  $5 \cdot 10^{-3} \text{ cm}^2 \text{ s}^{-1}$  for the preexponential factor a value of 1.0–1.1 eV is obtained. (The range for  $E_{diff}^*$  follows from the maximum and minimum diffusion times possible from the experiment. We mention that a more rigorous analysis by applying nucleation theory yields the same value for  $E_{diff}^*$ .)

Figure 2(c) shows a number of islands formed on the hot surface in more detail. The image was recorded after an exposure of 5 L of  $O_2$  at 470 K. The islands are hexagonal, with alternately longer and shorter sides. Within the islands a  $(1 \times 1)$  structure can be identified, i.e., the same structure as that formed at 300 K, and defects which will be discussed below. The alternating side lengths of the hexagons reflect the threefold rotational symmetry of a  $(1 \times 1)$  structure on an fcc(111) surface, by which, e.g., the number of oxygen atoms which coordinate an aluminum atom at the island borders are different at the long and short sides. This leads to different energies of the two different island edges or to different formation kinetics (e.g., the diffusion velocity of oxygen atoms along opposite edges may be different); both effects are known to cause similar shapes in other systems.<sup>23,24</sup> In any case, oxygen forms compact islands favoring straight edges, which evidences that significant attractive energies act between the oxygen atoms.

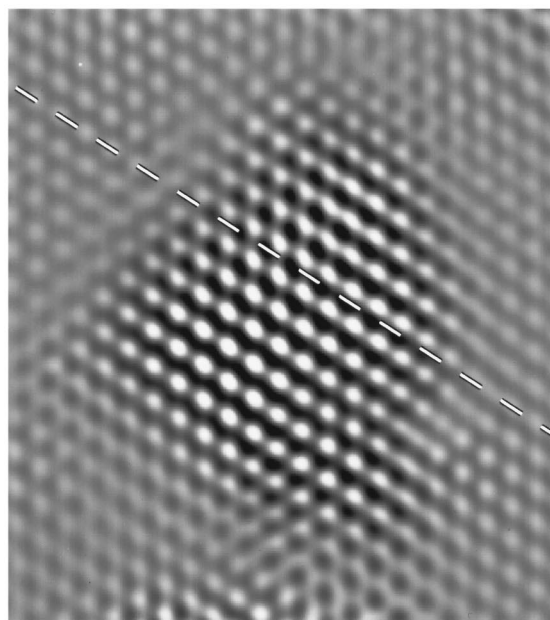
## B. Binding states of oxygen

By comparison with the room-temperature case<sup>2</sup> conclusions about the binding states of the oxygen atoms in the islands formed at elevated temperatures can be drawn. Figure 3(a) shows the internal structure of an island formed by exposure of 10 L of  $O_2$  at 470 K, which is typical for the low exposure regime treated so far. Similarly as in Fig. 2(c) the island, which is imaged 1.1 Å deep, displays a  $(1 \times 1)$  structure and additional defects. The  $(1 \times 1)$  structure became visible only for somewhat smaller tunnel resistances, between  $10^7$ – $10^9 \Omega$ , whereas the usually applied larger values revealed only depressions without an internal structure.

The image allows to identify the positions of the bright features within the  $(1 \times 1)$  structure relative to the positions of the surrounding Al atoms. The Al(111) substrate is actually atomically resolved in Fig. 3(a) but with a very small corrugation. By Fourier filtering the relative orientation of the  $(1 \times 1)$  lattice of the island with respect to the surrounding aluminum lattice is made visible [Fig. 3(b)]. [This was performed by multiplying the Fourier transform with a mask



(a)



(b)

FIG. 3. (a) Oxygen island after exposure of 10 L  $O_2$  at 470 K; arrows indicate oxygen atoms at the border which are imaged differently from those in the interior. (b) Same image after Fourier filtering,  $55 \text{ Å} \times 51 \text{ Å}$ ;  $-0.5 \text{ V}$ ,  $21 \text{ nA}$ .

consisting of Gaussians at the spots of the  $(1 \times 1)$  structure. One has to be careful not to choose too narrow Gaussians which would create a periodicity not contained in the original image. However, the fact that the information about extended anti-phase lattices of the  $(1 \times 1)$  structure is located in a narrow frequency range around the corresponding spots of the Fourier transform justifies this data evaluation.] The dashed line along a close packed row of aluminum atoms shows that the two lattices are out of phase. Assigning the protrusions on the bare metal to the aluminum atoms, the

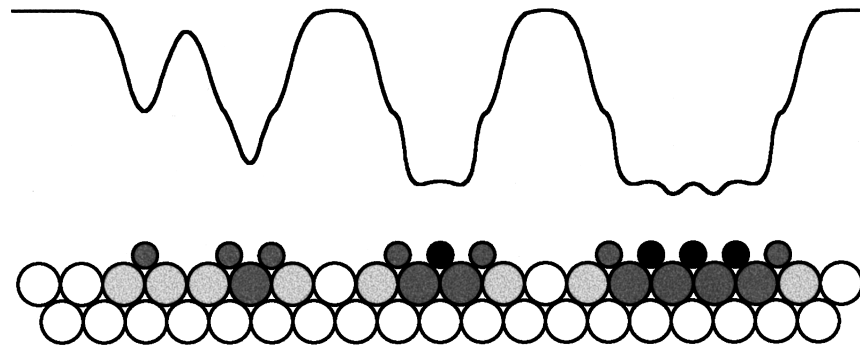


FIG. 4. Suggested STM profile over islands of different size. Shading indicates possible variations in the electron densities between interior and outer oxygen and aluminum atoms.

protrusions within the islands are on the positions of the threefold hollows of the aluminum. These are the most likely positions of the oxygen atoms. (Two recent studies, using standing x-ray absorption<sup>7</sup> and ion scattering,<sup>8</sup> identified the fcc hollow sites as the oxygen adsorption sites.) This means, in turn, that the oxygen atoms are imaged as small protrusions inside of deep holes. This finding is in qualitative agreement with the observation at 300 K<sup>2</sup> that at closer tip-sample distances, corresponding to resistances of  $10^6$ – $10^8 \Omega$ , central protrusions appear inside the oxygen holes. In the case of the higher temperature islands these become visible already at resistances about an order of magnitude larger.

An additional, quantitative difference concerning the imaging conditions to the 300 K data is the greater depth of the islands for the annealed surface. At room-temperature imaging depths of 0.6–1.0 Å are found, depending on the island size. The larger islands are imaged deeper, but no saturation was observed, apparently because the islands have not grown much larger than about 10 Å at the coverage at which the oxidation sets in Ref. 2. The islands in Figs. 2(c) and 3(a) have diameters of almost 30 Å and are flat at the bottom so that their imaging depth of 1.0–1.1 Å represents a saturation value. This suggests that the imaging of small oxygen islands by STM is dominated by the edges, at which the  $O_{ad}$  atoms are imaged less deep. This effect can indeed be seen for the islands formed at the higher temperatures; e.g., in Fig. 3(a) the  $(1 \times 1)$  protrusions at the island border (between the arrows) appear on a 0.3 Å higher level than those in the interior of the island.

We suggest that the STM tip follows contours over  $O_{ad}$  islands of varying sizes as sketched in Fig. 4. In agreement with the predicted reduced local density of states at  $E_F$ <sup>11</sup> the adsorption complex, consisting of the  $O_{ad}$  atom and the surrounding Al atoms, is imaged as a depression; the depth depends, however, on the island size. For smaller tip-sample distances a central protrusion at the position of the oxygen atom appears which is resolved more easily for larger islands. Both effects are therefore related to the coordination number of the oxygen atoms. This may be explained by a resolution effect emerging from the fact that the charge density of the tip is laterally smeared out. At the island borders, where the charge density might change quite rapidly, the

STM will then average over the oxygen atoms and the bare metal; small islands may be dominated by such an effect. Alternatively, it may be a genuine effect of the sample, caused by variations of the electron density of the adsorption complexes with the number of oxygen neighbors. From the extremely strong chemical interaction between the oxygen atom and the aluminum surface such differences can be expected because of the small lattice constant of the  $(1 \times 1)$  structure. Such effects have actually been observed by photoemission spectroscopy where both the  $Al(2p)$ <sup>25</sup> and the  $O(1s)$ <sup>26</sup> core levels showed energy shifts resulting from differently coordinated  $O_{ad}/Al$  complexes. In any case, the variations in STM imaging of the  $(1 \times 1)$  islands formed at 300 K vs those at elevated temperatures, which were quite confusing in the beginning, can be consistently explained by a size effect. We conclude, therefore, that the  $(1 \times 1)$  structures formed at room temperature and at higher temperatures consist of the same oxygen species; hence, at temperatures up to 470 K, and for exposures up to 10 L, a considerable part of the oxygen still exists in the form of chemisorbed atoms.

The images show additional structures that are different from the  $(1 \times 1)$  phase. One can discriminate bright spots at the borders between the islands and the bare aluminum surface [Figs. 1(a) and 3(a)], corresponding to protrusions with an apparent height of about 1 to 2 Å, and defects within the  $(1 \times 1)$  structure [Figs. 2(c) and 3(a)]. As already mentioned [Figs. 2(c) and 3(a)], the bright features closely resemble the small bright grains occurring at 300 K for  $\Theta > 0.2$  at step edges and at the borders of  $O_{ad}$  islands. By simultaneous observation of the oxidic  $Al_{LVV}$  AES peak at 54 eV,<sup>2</sup> these had been identified as aluminum oxide nuclei at 300 K. For the disordered areas within the islands it is also very likely that they represent some form of oxide, where the different appearance might be caused by a different stoichiometry or different structure. In order to form the ordered, stoichiometric  $Al_2O_3$  extensive site exchange processes between oxygen and aluminum atoms have to take place, making it likely that intermediates occur. This assignment is consistent with results from previous annealing experiments or adsorption experiments at elevated temperatures where in all cases the spectroscopic features characteristic of the oxidic species appeared.<sup>12–18</sup> The

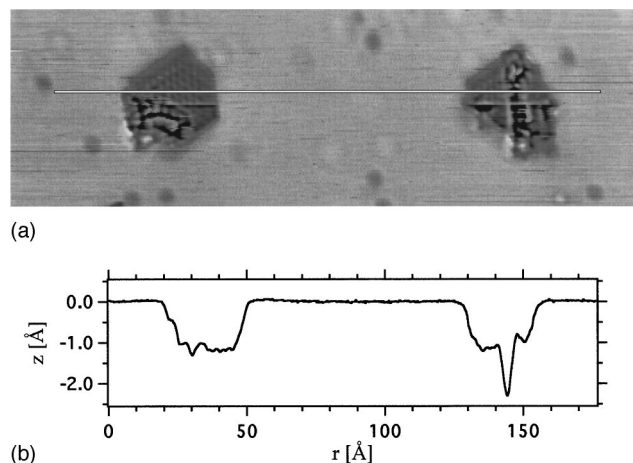


FIG. 5. (a) Oxygen islands after exposure of 3 L O<sub>2</sub> at 440 K. 210 Å × 67 Å; -0.9 V, 3 nA. (b) Profile along the line marked in (a).

absence of the Al<sup>3+</sup> AES peak in the present study is explained by the small exposures applied.

The interpretation of the STM data at elevated temperatures is, however, complicated by a further feature. This becomes evident from Fig. 5(a) showing two of the typical islands containing the (1 × 1) structure and disordered areas. The profile [Fig. 5(b)] along the marked line shows at one location within the disordered area a more than 2 Å deep hole that is clearly different from the 1.1 Å deep, flat (1 × 1) areas. Such holes are often observed also in other islands. Figure 6 depicts a histogram of the number of islands in Fig. 2(a), for which the deepest point in each of the islands was determined. [Since most of the islands contain deeper holes than the 1.1 Å deep (1 × 1) structure there is no peak corresponding to this structure in the histogram.] There is a clear peak at 2.3 Å which is exactly the layer distance of the Al(111) substrate. Also a peak corresponding to the second layer seems to evolve. That the full depth of 4.7 Å is not reached might be caused by the finite tip diameter which prevents the tip from “seeing” the bottom of the holes that are often less than 6 Å wide. One is therefore tempted to ascribe these features to actual topographic hollows and not to an electronic effect like that responsible for the imaging of the chemisorbed O<sub>ad</sub>.

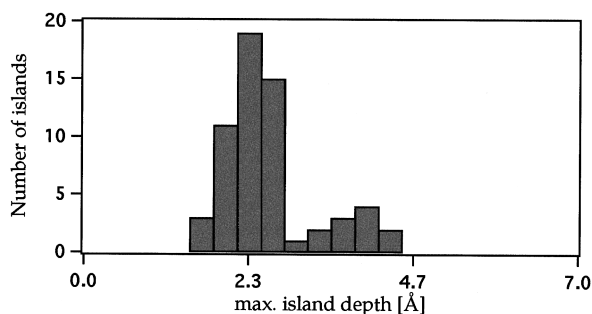


FIG. 6. Histogram of the number of islands in Fig. 2(a) with respect to their maximum imaging depth.

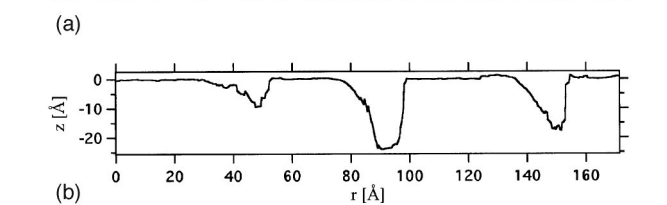
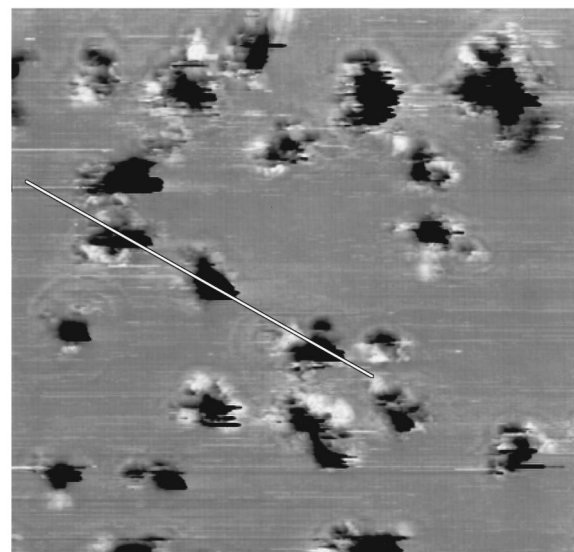


FIG. 7. (a) STM topograph of Al(111) recorded after exposure of 20 L O<sub>2</sub> and 5 min. annealing at 515 K. 266 Å × 212 Å; -0.37 V, 20 nA. (b) Profile along the line indicated in (a).

In fact holes as deep as 20 Å were observed after larger exposures and subsequent annealing. Figure 7(a) shows an STM topograph recorded after exposure of 20 L and annealing at 515 K for 5 min. The (1 × 1) islands have disappeared, the dark features surrounded by bright rims correspond to holes which are mostly between 10 and 20 Å deep [Fig. 7(b)]. The larger holes are deeper than the tip-sample distance which is usually assumed to be between 5 and 10 Å.<sup>27</sup> This rules out an interpretation in terms of an electronic effect alone and seems to support the notion of topographic holes.

However, topographic holes indicate the removal of Al atoms which can be reasonably explained only when this material is consumed by oxide grains growing somewhere on the surface. At the exposure applied in the experiment of Fig. 7 sizeable Al oxide particles should therefore be detected, which, because of the lower density (of Al atoms per volume element) of Al<sub>2</sub>O<sub>3</sub> compared to metallic Al, should even protrude above the surface. However, at this exposure no other features than those visible in Fig. 7(a) were observed, and the bright rims around the holes in Fig. 7(a) are too flat to account for the “missing” material, indicating that the holes themselves are connected with the oxide. A possible, although speculative, interpretation is that the holes are actually filled with Al oxide and that the apparent topography seen by the STM represents only the contours of the metal cavities in which the oxide grains are embedded. That the oxide does not contribute to the tunnel current can be explained when it is better ordered than the oxide features de-

scribed above and already nonconducting. This would explain the peak corresponding to the Al layer spacing in the histogram of Fig. 6. For the deep holes of Fig. 7 this interpretation implies, however, that the tip would make mechanical contact on the oxide grains before reaching the metal underneath. This may account for the tip instabilities over the hole features, reflected by their noisy borders in Fig. 7(a), although we do not have an explanation so far, why such an effect should not lead to larger damages of the tip.

#### IV. CONCLUSIONS

1. By annealing an Al(111) surface, precoversed with small amounts of oxygen at 300 K, to temperatures between 350 and 530 K, or by adsorption in this temperature range, thermally activated processes are observed: The chemisorbed oxygen atoms become mobile, and larger  $(1 \times 1)O_{ad}$  islands are formed either by a direct nucleation and growth process (adsorption at elevated temperatures) or by Ostwald ripening (post annealing). This contrasts very much the nonadiabatic kinetics at 300 K.<sup>2</sup> The thermal growth of the  $(1 \times 1)O_{ad}$  islands at 350–530 K demonstrates that it is possible to anneal the surface covered with small amounts of  $O_{ad}$  without direct, full transformation of the—metastable—chemisorbed oxygen into the thermodynamically stable oxide. This had not been found in previous studies in which, upon annealing, the electronic<sup>12–16</sup> and vibrational spectra<sup>17,18</sup> displayed directly the characteristics of aluminum oxide. This may be explained by the larger exposures (30–100 L) applied there (except in one HREELS study,<sup>17</sup> in which the exposure scale deviates, however, from the other studies also at 300 K<sup>2</sup>).

2. The results allow to draw conclusions about the energies that play a role in the interaction between oxygen and the Al(111) surface:

- ◆ For the diffusion barrier of the chemisorbed oxygen a value of 1.0–1.1 eV was evaluated, in agreement with the lower limit of 1.0 eV derived in a previous paper.<sup>2</sup> It is also roughly in accordance with calculated values between 0.75 and 0.8 eV for the binding energy difference between an oxygen atom on the fcc site and the bridge position,<sup>5</sup> corresponding to the minimum energy an atom has to overcome to jump from one fcc site to a neighboring one. Although the value for the diffusion barrier appears quite large it is within the usual 10–20% range of the adsorption energy (with respect to the free atom) that is typical for atomic adsorbates.<sup>6,28,29</sup> A recent calculation<sup>5</sup> determined a binding energy of 5.0 eV/atom with respect to  $O_2$ , corresponding to 7.6 eV/atom with respect to the free atom.
- ◆ Like at room temperature, the  $(1 \times 1)O_{ad}$  phase formed at elevated temperatures is imaged by the STM as a depression, in agreement with the reduced LDOS (local density of states) at  $E_F$  predicted for an oxygen atom on a jellium surface.<sup>11</sup> The additional protrusions inside the depressions at the positions of the oxygen atoms, which appear at closer tip-to-sample distances, could also be confirmed in a recent theoretical study.<sup>5</sup> There are quantitative differences with respect to the imaging of the room-

temperature  $(1 \times 1)$  structure (a greater depth of the depressions and the appearance of the central protrusions already at larger tunnel resistances) which are explained, however, by a size effect: The  $O_{ad}$  atoms at the borders of the islands are imaged differently from those in the interior by which the small room-temperature islands appear differently from the larger islands formed at higher temperatures. Similarly to 300 K there is no indication for a second chemisorbed oxygen species, which has been discussed in the past in connection with a subsurface site. Also the diffusion barrier that was obtained here is consistent with a surface site. Since in most theoretical studies the subsurface position is found to be energetically lower (e.g., by 1.86 eV in Ref. 5) there must be a sizeable activation barrier between the surface and the subsurface sites. A lower limit is given by  $E_{diff}^* = 1.0$  eV since surface diffusion of  $O_{ad}$  could be induced by annealing. That subsurface sites are not populated is suggested to be caused by the competing oxide formation.

- ◆ The fact that  $(1 \times 1)$  islands grow by annealing is direct evidence for attractive interactions between the adsorbed oxygen atoms. Because of the thermal immobility at 300 K this could not be concluded with certainty from the previous data.<sup>2</sup> The small  $(1 \times 1)$  clusters observed at room temperature do not form thermally, by attachment of diffusing oxygen atoms, but result from the dissociation of the molecules (a capture of ‘hot atoms’ which release their energy at atoms that are already equilibrated had been suggested).<sup>2</sup> These data left therefore the possibility that the  $(1 \times 1)$  structure is only metastable with respect to other structures. For transition metal surfaces the most stable oxygen structures are more open, whereas overlayers with smaller lattice constants, that are found in some cases at larger exposures, do not form islands on the bare surface; typical examples are the  $(2 \times 2)$  and  $(2 \times 1)$  overlayers on Ru(0001).<sup>30,31</sup> (The  $(1 \times 1)$  structure prepared recently on this surface was obtained only by using  $NO_2$ .)<sup>32,33</sup> Attractive nearest-neighbor interactions between  $O_{ad}$  underlying the formation of the  $(1 \times 1)$  structure on Al(111) is therefore an important result. It is supported by a recent density functional calculation<sup>5</sup> in which the  $(1 \times 1)$  structure was found to be by 0.5 eV/atom more stable than a  $(2 \times 2)$  structure, which was explained by the unusual strength of the Al–O bond.

3. The interpretation of the conversion of the chemisorbed oxygen into aluminum oxide is complicated by the observation of several different features in the STM images, in addition to the  $(1 \times 1)$  islands. The data can, however, be explained consistently if these represent different stages of the oxidation. The first step is a local transformation within the  $(1 \times 1)$  islands of chemisorbed oxygen, caused by site exchange processes between the oxygen and Al atoms (at this point oxygen atoms must, in fact, move to subsurface positions). In a later stage these nuclei order into  $Al_2O_3$  which is nonconducting and transparent to the STM. These conversions take place already after an exposure of 3 L at 440 K, in

contrast to room temperature where oxidation started only at about  $60 \text{ L O}_2^{-2}$  which underlines the fact that the  $(1 \times 1)$  phase is only metastable with respect to the oxide. A further result is that the oxidation develops also at nondefect sites (on the terraces), which results from the conversion of chemisorbed oxygen islands into oxide. The distribution of the oxide nucleation sites is, therefore, not an intrinsic property of the oxidation, but results from the (mostly) homogeneous nucleation of the  $\text{O}_{\text{ad}}$  islands.

- <sup>1</sup>H. Brune, J. Winterlin, R. J. Behm, and G. Ertl, *Phys. Rev. Lett.* **68**, 624 (1992).
- <sup>2</sup>H. Brune, J. Winterlin, J. Trost, G. Ertl, J. Wiechers, and R. J. Behm, *J. Chem. Phys.* **99**, 2128 (1993).
- <sup>3</sup>C. Engdahl and G. Wahnström, *Surf. Sci.* **312**, 429 (1994).
- <sup>4</sup>G. Wahnström, A. B. Lee, and J. Strömqvist, *J. Chem. Phys.* **105**, 326 (1996).
- <sup>5</sup>J. Jacobsen, B. Hammer, K. W. Jacobsen, and J. K. Nørskov, *Phys. Rev. B* **52**, 14954 (1995).
- <sup>6</sup>E. G. Seebauer and C. E. Allen, *Prog. Surf. Sci.* **49**, 265 (1995).
- <sup>7</sup>M. Kerkar, D. Fischer, D. P. Woodruff, and B. Cowie, *Surf. Sci.* **271**, 45 (1992).
- <sup>8</sup>E. R. Wouters, D. J. O'Connor, J. F. van der Veen, P. M. Zagwijn, J. Vrijmoeth, W. Slijkerman, and J. W. M. Frenken, *Surf. Sci.* **296**, 141 (1993).
- <sup>9</sup>I. P. Batra and L. Kleinman, *J. Electron Spectrosc. Relat. Phenom.* **33**, 175 (1984).
- <sup>10</sup>M. Schmid, W. Hebenstreit, P. Varga, and S. Crampin, *Phys. Rev. Lett.* **76**, 2298 (1996).
- <sup>11</sup>N. D. Lang, *Comments Condens. Matter Phys.* **14**, 253 (1989).
- <sup>12</sup>A. M. Bradshaw, P. Hofmann, and W. Wyrobisch, *Surf. Sci.* **68**, 269 (1977).
- <sup>13</sup>S. A. Flodström, C. W. B. Martinsson, R. Z. Bachrach, S. B. M. Hagström, and R. S. Bauer, *Phys. Rev. Lett.* **40**, 907 (1978).
- <sup>14</sup>A. Bianconi, R. Z. Bachrach, S. B. M. Hagström, and S. A. Flodström, *Phys. Rev. B* **19**, 2837 (1979).
- <sup>15</sup>W. Eberhardt and F. Himpsel, *Phys. Rev. Lett.* **42**, 1375 (1979).
- <sup>16</sup>D. Norman, S. Brennan, R. Jaeger, and J. Stöhr, *Surf. Sci.* **105**, L297 (1981).
- <sup>17</sup>J. L. Erskine and R. L. Strong, *Phys. Rev. B* **25**, 5547 (1982).
- <sup>18</sup>J. E. Crowell, J. G. Chen, and J. T. Yates, Jr., *Surf. Sci.* **165**, 37 (1986).
- <sup>19</sup>B. G. Frederick, M. B. Lee, and N. V. Richardson, *Surf. Sci.* **348**, L71 (1996).
- <sup>20</sup>P. H. Holloway and R. A. Outlaw, *Surf. Sci.* **111**, 300 (1981).
- <sup>21</sup>J. A. Venables, G. D. T. Spiller, and M. Hanbücken, *Rep. Prog. Phys.* **47**, 399 (1984).
- <sup>22</sup>B. Chalmers, *Physical Metallurgy* (Wiley, New York, 1959).
- <sup>23</sup>C. Herring, *Phys. Rev.* **82**, 87 (1951).
- <sup>24</sup>T. Michely, M. Hohage, M. Bott, and G. Comsa, *Phys. Rev. Lett.* **70**, 3943 (1993).
- <sup>25</sup>C. F. McConville, D. L. Seymour, D. P. Woodruff, and S. Bao, *Surf. Sci.* **188**, 1 (1987).
- <sup>26</sup>P. S. Bagus, C. R. Brundle, F. Illas, F. Parmigiani, and G. Polzonetti, *Phys. Rev. B* **44**, 9025 (1991).
- <sup>27</sup>J. K. Gimzewski and R. Möller, *Phys. Rev. B* **36**, 1284 (1987).
- <sup>28</sup>J. Winterlin, R. Schuster, and G. Ertl, *Phys. Rev. Lett.* **77**, 123 (1996).
- <sup>29</sup>T. Zambelli, J. Trost, J. Winterlin, and G. Ertl, *Phys. Rev. Lett.* **76**, 795 (1996).
- <sup>30</sup>M. Lindroos, H. Pfnür, G. Held, and D. Menzel, *Surf. Sci.* **222**, 451 (1989).
- <sup>31</sup>H. Pfnür, G. Held, M. Lindroos, and D. Menzel, *Surf. Sci.* **220**, 43 (1989).
- <sup>32</sup>I. J. Malik and J. Hrbek, *J. Vac. Sci. Technol. A* **10**, 2565 (1992).
- <sup>33</sup>C. Stampfl, S. Schwegmann, H. Over, M. Scheffler, and G. Ertl, *Phys. Rev. Lett.* **77**, 3371 (1996).